Available online at www.sciencedirect.com
SCIENCE DIRECT®
International Journal of Heat and Mass Transfer 48 (2005) 1868–1873
International Journal of HEAT and MASS TRANSFER
www.elsevier.com/locate/ijhmt

Technical Note

Droplet vaporization model in the presence of thermal radiation

B. Abramzon [a], S. Sazhin [b,*]

[a] ELOP Electro-Optics Industries Ltd., P.O. Box 1165, Rehovot 76111, Israel
[b] School of Engineering, Faculty of Science and Engineering, The University of Brighton, Brighton BN2 4GJ, UK

Received 5 March 2004; received in revised form 29 November 2004

1. Introduction

Accurate modeling of droplet vaporization is essential in many practical engineering applications including diesel engines [1]. In practice, there is a considerable gap between the 'state of the art' models developed by various research groups [2,3] and the simpler models used in CFD codes [4]. The model developed in [2] combines accuracy and computer efficiency, which enables its application in practical spray combustion calculations. It takes into account many important effects, such as: variable physical properties and non-unitary Lewis number in the gas phase; influence of the Stefan flow (blowing) on heat and mass transfer and hydrodynamics drag; and, the effect of the transient liquid heating inside the droplet. The effect of internal circulation on heat transfer in a droplet is simulated using two models: (a) the 'extended model' which directly solves the convective energy equation inside the droplet and (b) the 'effective conductivity model' which assumes that heat is transferred within the droplet by thermal conduction with some 'effective' coefficient of thermal conductivity of the liquid, k_{eff}. In the present paper, both the 'extended model' and 'effective conductivity model' [2] are developed further to take into account the effect of radiative heating of droplets and variable physical properties of the liquid, including how liquid density varies with droplet temperature (thermal expansion).

The effect of radiation absorption on the heating and evaporation processes of a single droplet has been studied in many papers. Lage and Rangel [5] based their analysis on Mie theory. Although the model for radiative heating of droplets used in [5] is accurate, its practical applications in CFD codes are limited due to its complexity. In the present study, the radiation absorption model suggested by Dombrovsky and Sazhin [6] is used. This model takes into account the distribution of thermal radiation absorption inside droplets, but its formulation is much simpler than that of the model used in [5]. Modeling of the radiative heating of droplets in this paper will be essentially based on the model developed in [6].

2. Description of the model

The algorithm for calculating the absorption of thermal radiation, suggested in [6] is based on the assumptions that droplets are spherical and semi-transparent, their irradiation is spherically symmetric and the geometric optics approximation is valid (i.e. the size parameter is considerably greater than 1). The calculations require knowledge of the spectral optical properties of the liquid fuel: index of absorption $\kappa_\lambda = \kappa(\lambda)$, and refractive index $n = n(\lambda)$. The former was measured experimentally in the range of wavelengths 0.2–6 μm, while the latter was calculated from the measured index of absorption κ_λ using the subtractive Kramers–Krönig analysis.

The simplified models for droplet vaporization suggested in [2] have been enhanced to take into account the thermal radiation absorption effect, using the approach

* Corresponding author.

0017-9310/$ - see front matter
doi:10.1016/j.ijheatmasstransfer.2004.11.017

described in [6], and temperature dependence of physical properties in the liquid phase. One of the main assumptions of these models is that the droplet surface temperature is uniform but varies with time. This assumption reduces the dimension of the problem and allows separation of the calculations referring to the gas and liquid phases. The analysis of the gas phase is the same as described in [2], but some modifications are introduced in the analysis of the liquid phase to take into account the effect of thermal radiation and variable physical properties of the liquid.

The temperature, T, within the droplet, taking into account the effect of internal liquid circulation, is governed by the equation:

$$\frac{\partial}{\partial t}(\rho_L C_{pL} T) + \rho_L C_{pL}(\boldsymbol{V}\cdot\nabla)T = \nabla\cdot(k_L \nabla T) + Q, \tag{2.1}$$

where Q is the volumetric heat source in [W/m^3], representing the thermal radiation absorption rate per unit volume, $\boldsymbol{V}$ is the fluid velocity vector within the droplet. Introduction of the term Q is the new element of the model.

The physical properties of the liquid, such as density ρ_L, specific heat capacity C_{pL}, thermal conductivity k_L and dynamic viscosity μ_L, depend on the local temperature. The standard practice is to evaluate the liquid properties at some reference temperature, $T_{ref} = A\times(T_0 + T_{boil})$, where A is close to 0.5. Based on the theoretical analysis of the diffusion controlled evaporation of a multicomponent fuel droplet, Kneer et al. [7] recommended to estimate the above reference temperature with $A = 0.55$–0.6 (cf. the analysis reported in [8]). In the present study, the temperature dependence of the liquid properties is taken into account. However, to simplify the problem, it is assumed that these properties may be evaluated at the volume-averaged droplet temperature, T_{av}, which varies with time. In addition, it appears that for many fuels the liquid specific heat capacity increases with the temperature, so the temperature dependence of the product $(\rho_L C_{p,L})$ is relatively weak. Thus, for n-decane and n-dodecane fuels used in the present study, the variation of $(\rho_L C_{p,L})$ does not exceed 10% within the temperature range between 300 and 600 K. Hence, the product $(\rho_L C_{p,L})$ in the first term of LHS of Eq. (2.1) can be considered as a constant value within the droplet. Assuming that the internal streamlines of the liquid circulating within the droplet follow a spherical Hill vortex pattern, the dimensionless energy equation is expressed as:

$$\varphi^2\frac{\partial Z}{\partial t_L} + [0.5 Pe_L \varphi V_r - \beta\eta]\frac{\partial Z}{\partial \eta} + 0.5 Pe_L \frac{V_\theta \varphi}{\eta}\frac{\partial Z}{\partial \theta} = \frac{1}{\eta^2}\frac{\partial}{\partial \eta}\left(\eta^2\frac{\partial Z}{\partial \eta}\right) + \frac{1}{\eta^2\sin\theta}\frac{\partial}{\partial\theta}\left(\sin\theta\frac{\partial Z}{\partial\theta}\right) + \varphi^2 q(\eta,\theta), \tag{2.2}$$

where $Z = T/T_0$ is a non-dimensional temperature; T_0 is the droplet initial temperature; $\varphi = R_d/R_{d0}$ is the instantaneous radius of the droplet related to it's initial radius; θ is the angular coordinate; $V_r = (1-\eta^2)\cos\theta$, $V_\theta = (1-2\eta^2)\sin\theta$ are the non-dimensional fluid velocity components of the Hill vortex [9]. $t_L = \alpha_L t/R_{d0}^2$ is the non-dimensional time; α_L is the liquid thermal diffusivity; $q(\eta,\theta) = R_{d0}^2 Q/(k_L T_0)$ is the non-dimensional volumetric heat source. The liquid Peclet number, $Pe_L = 2U_s R_{d0}/\alpha_L$, is based on the maximum surface velocity, which may be estimated as [2]: $U_s = \frac{1}{32}U_{rel}(\frac{\mu_g}{\mu_L})Re_g C_F(Re_g)$, where C_F is the friction drag coefficient, estimated as:

$$C_F = \frac{12.69}{Re_g^{2/3}(1+B_M)}. \tag{2.3}$$

Expression (2.3) combines the correlation of numerical data presented in [9] for C_F of a solid non-vaporizing sphere in the range of $10 < Re_g < 100$ with the correction $1/(1+B_M)$ introduced in [10] to take into account the influence of the Stefan flow. The non-dimensional parameter β is proportional to the regression rate of the droplet surface:

$$\beta = -\frac{1}{2}\frac{d(\varphi^2)}{dt_L} \equiv -\frac{1}{2\alpha_L}\frac{dR_d^2}{dt}. \tag{2.4}$$

The term β can be related to the vaporization rate:

$$\dot m = -\frac{d}{dt}\left(\frac{4}{3}\pi\rho_L R_d^3\right) \equiv -2\pi R_d \rho_L \frac{d(R_d)^2}{dt} - \frac{m}{\rho_L}\left(\frac{d\rho_L}{dT_{av}}\right)\left(\frac{dT_{av}}{dt}\right). \tag{2.5}$$

The temporal variation of the droplet mean temperature may be approximately expressed as:

$$mC_{p,L}\frac{dT_{av}}{dt} \approx Q_L + Q_{rad,tot}, \tag{2.6}$$

where Q_L is the heat penetrating into the droplet by convection and conduction from the gas phase, and $Q_{rad,tot}$ is the total radiation absorption by the droplet. Finally, combining Eqs. (2.5) and (2.6), one obtains:

$$\beta = -\frac{1}{4\pi\alpha_L\rho_L R_d}\left[\dot m + \frac{1}{\rho_L C_{p,L}}(Q_L + Q_{rad,tot})\right]. \tag{2.7}$$

The energy equation (2.2) is solved under the standard initial and boundary conditions [2], supplemented by the conditions at the droplet surface

$$\eta = 1, \quad \partial Z/\partial\theta = 0, \tag{2.8}$$

$$\int_0^\pi \left(\frac{\partial Z}{\partial\eta}\right)\sin\theta\, d\theta = \frac{Q_L}{2\pi R_d k_L T_0}. \tag{2.9}$$

Eqs. (2.1)–(2.9) represent the so-called 'extended' model of heat transfer within the circulating liquid droplet. This model can be considered to be the most accurate

among the simplified liquid-phase models such as the 'infinite-conductivity', 'conduction-limit', or 'vortex' models [3]. However, due to the computational complexity, the 'extended' model is not suitable to be employed in the spray combustion CFD codes. The use of the 'extended' model in the present study was motivated by the findings of [11] that the effect of radiation absorption for *n*-decane droplet may be as important as the choice of the liquid-phase model.

The energy equation for the so-called 'effective thermal conductivity' model [2,3] is obtained from the 'extended' model equation (2.1) by setting $\partial/\partial\theta = 0$; $V_r = V_\theta = 0$:

$$\varphi^2 \frac{\partial Z}{\partial t_L} = \beta\eta \frac{\partial Z}{\partial \eta} + \frac{1}{\eta^2}\frac{\partial}{\partial \eta}\left(\eta^2 \frac{\partial Z}{\partial \eta}\right) + \varphi^2 Q(\eta, \theta) \tag{2.10}$$

and multiplying the thermal conductivity of the liquid by the factor χ which reflects the effect of internal circulation on heat transfer within the droplet: $k_{L,\mathrm{eff}} = \chi \cdot k_L$. The factor χ varies within the range of 1–2.72 depending on the instantaneous liquid Peclet number [2]. Eq. (2.10) is solved under the standard initial condition [2] and the boundary conditions:

$$\begin{cases} \eta = 0 & \partial Z/\partial\eta = 0; \\ \eta = 1 & \partial Z/\partial\eta = Q_L/(4\pi R_d k_L T_0). \end{cases} \tag{2.11}$$

The droplet velocity and position at time $(t + \Delta t)$ are evaluated using the equations [3]:

$$\frac{d\vec{X}}{dt} = \vec{U}, \tag{2.12}$$

$$\frac{d\vec{U}}{dt} = -\frac{3C_D(Re_g, B_m)}{8R_d}\left(\frac{\rho_\infty}{\rho_L}\right)\cdot|\vec{U} - \vec{U}_\infty|\cdot(\vec{U} - \vec{U}_\infty). \tag{2.13}$$

Following [10,12] the drag coefficient of the evaporating droplet may be approximated by the 'standard drag curve' for a solid sphere provided that the droplet Reynolds number is defined as: $Re_g = 2U_{rel}\rho_g R_d/\mu_g$. The droplet radius is calculated from Eq. (2.4). The numerical method used in the present study is essentially the same as in [2]. It should be emphasized that in both the 'extended' and the 'effective-conductivity' models, the physical properties of the liquid and the liquid Peclet number are updated at each time-step. Hence, the value of the non-dimensional time-step, $\Delta t_L = \alpha_L \Delta t/R_{d0}^2$, in Eqs. (2.1) and (2.9), varies even if the dimensional time step Δt is constant.

3. Results and discussion

The calculations have been performed for two types of fuels: *n*-decane and low sulfur ESSO AF1313 diesel fuel used in cars. Data for the index of absorption of *n*-decane was taken from [13], while data for the low sulfur ESSO AF1313 diesel fuel was taken from the original measurements, as reported in [6]. More accurate measurements of κ reported in [14] are not expected to influence significantly the results of our analysis.

Comparison of our results for radiation absorption in *n*-decane droplets with Figs. 10 and 11 of [5] shows general agreement between the predictions of our simplified model and the predictions of Mie theory for *n*-decane for the same values of input parameters, although some minor details of the plots are different. Peaks of absorption near the droplet surfaces predicted by the simplified model and the general Mie theory appear to be almost the same for all droplets. The results for diesel fuel are reasonably close to those presented in Fig. 5a of [6]. The difference between the actual values of the absorbed radiative power (not exceeding 10% in most cases) can be attributed to the fact that [6] used a rough approximation of the index of absorption, while in our case the experimentally measured values of this index were used.

Calculations of the vaporization history of droplets, heated by convection and radiation, were performed using the finite-difference approach with the grid having 100 cells in the radial directions and 90 cells in the angular directions. The time step was about 0.01 ms. Grid independence of the solution was verified by comparison with the results obtained with a 50×60 grid. The difference in the evaporation rate predicted by the two solutions did not exceed 0.1%. The calculations of the droplet vaporization history were performed for two cases. The first case corresponds to the conditions considered previously by Lage and Rangel [11]: *n*-decane droplet of initial radius $R_{d0} = 50$ μm and temperature $T_0 = 300$ K is inserted into a hot air flow at $T_\infty = 1000$ K and $p_\infty = 10$ bar. The initial droplet velocity relative to the gas was set $U_{rel} = 8$ m/s which corresponds to an initial Reynolds number of about 100. The black-body temperature responsible for the radiative heating of droplets, T_{ext}, is set at 1000, 1250 and 1500 K. The second case is focused on the vaporization of the above-mentioned diesel fuel at conditions close to those of diesel engines: $p_\infty = 30$ bar and $T_\infty = 750$ K. The initial droplet parameters are: radius $R_{d0} = 50$ μm, velocity is $U_{rel} = 15$ m/s, and the temperature is $T_0 = 300$ K. In both cases, the droplet temperature remained below the critical temperature of the liquid in course of evaporation. The difference between T_∞ and T_{ext} is typically observed in the case when droplets are injected into a relatively cold gas, but are heated by thermal radiation from remote hot flame [15]. Contrary to *n*-decane, the physical properties of diesel fuels are not available in the open literature. Therefore, in the present study it was assumed that these properties can be approximated by those of *n*-dodecane [15]. In what follows 'diesel fuel' is understood to mean a fuel having

the physical properties of *n*-dodecane and the radiation absorption properties of low sulfur ESSO AF1313 diesel fuel.

As follows from our calculations for a *n*-decane droplet based on the 'extended' model at different values of the black-body temperature T_{ext}, the droplet heating at the initial stage causes an increase in droplet radius due to the thermal expansion of the liquid. The radiation absorption has a relatively small effect on the droplet vaporization history, in agreement with [11].

Unlike *n*-decane droplets, the effect of radiation absorption is much more pronounced for diesel fuel droplets. Fig. 1 shows the effect of T_{ext} (thermal radiation) on the decrease of the normalized droplet radius due to evaporation. As can be seen from this figure, an increase in T_{ext} from 1000 K to 1500 K leads to a decrease in evaporation time of more than 30%. The difference between the effects of thermal radiation on evaporation times of *n*-decane and diesel fuel can be attributed to the fact that the absorption of thermal radiation by diesel fuel is much greater than that of *n*-decane The time evolution of the normalized vaporization rate for diesel fuel at various T_{ext} is shown in Fig. 2. This variable is most sensitive to various parameter variations. Initially, the vaporization rate increases with time, as the droplet is heated-up. The following decrease in the vaporization rate is related to the decrease of droplet radius. As expected, the maximum vaporization rate increases with increasing T_{ext}. In the same figure, the dotted curves show the calculations made under the assumption that the internal heat sources due to the radiation absorption are uniformly distributed over the droplet volume: $Q(r) = 3Q_{rad,tot}/(4\pi R_d^3)$. As can be seen from this figure, the assumption of uniform radiation absorption yields very good agreement with the more detailed model. A similar observation was previously made in [11] for *n*-decane droplets. This is as expected—the total effect of radiation for *n*-decane is small. Assuming uniform radiation absorption allows reduction in total computation time. The total radiation absorbed by the droplet may be evaluated using the relation [6]:

$$Q_{rad,tot} = 4\pi^2 R_d^2 \int_{\lambda_1}^{\lambda_2} E_a B_\lambda(T_{ext})\,d\lambda, \tag{3.1}$$

where

$$E_a = \frac{4n_\lambda}{(n_\lambda+1)^2}[1-\exp(-8\pi\kappa_\lambda R_d/\lambda)]$$

and

$$B_\lambda(T_{ext}) = \frac{C_1}{\pi\lambda^5[\exp(C_2/(\lambda T_{ext})-1)]},$$

$C_1 = 3.742$ W μm^4/m^2, $C_2 = 1.439\times10^4$ μm K, λ is the wavelength in μm.

Based on experimental data for diesel fuels, Dombrovsky and Sazhin [6] suggested that the averaged (over wavelengths) absorption efficiency factor, $\overline{E}_a$, of semi-transparent droplets can be approximated as $\overline{E}_a = aR_d^b$, where R_d is the droplet radius, a and b are polynomials of the external temperature (see also [14]). Using this value, the total radiation heat absorption by the droplet is calculated as: $Q_{rad,tot} = 4\pi R_d^2 \sigma \overline{E}_a T_{ext}^4$.

In absence of radiation, the droplet temperature approaches some equilibrium or 'wet-bulb' temperature which is about 600 K for the present case. At that

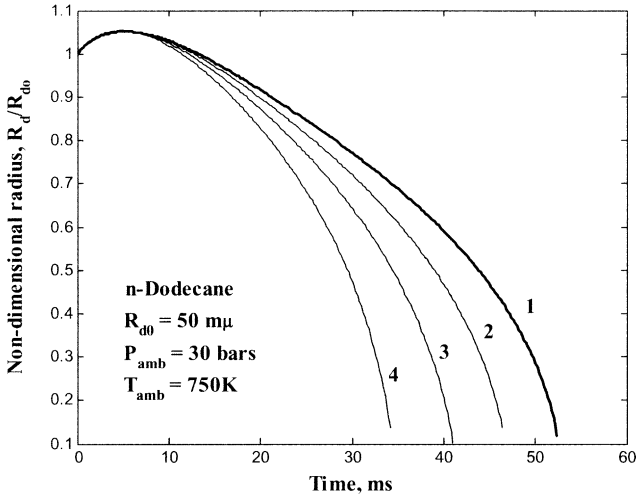

Fig. 1. Normalized radius of a diesel fuel (*n*-dodecane) droplet versus time at various external temperatures, T_{ext}, as predicted by the 'extended' model with the distributed radiation absorption, for $R_{d0} = 50$ μm, $T_0 = 300$ K, $T_\infty = 750$ K, $p_\infty = 30$ bar and $U_{rel,0} = 15$ m/s. Curve 1 refers to the case without radiation; curve 2 refers to the case when $T_{ext} = 1000$ K; curve 3 refers to the case when $T_{ext} = 1250$ K; curve 4 refers to the case when $T_{ext} = 1500$ K.

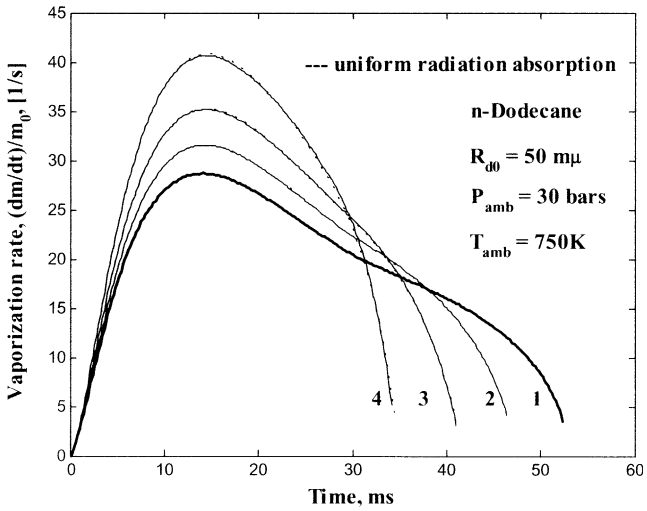

Fig. 2. Normalized vaporization rate of a diesel fuel (*n*-dodecane) droplet versus time at various external temperatures, T_{ext}, as predicted by the 'extended' model with the distributed radiation absorption, for $R_{d0} = 50$ μm, $T_0 = 300$ K, $T_\infty = 750$ K, $p_\infty = 30$ bar and $U_{rel,0} = 15$ m/s. Curve 1 refers to the case without radiation; curve 2 refers to the case when $T_{ext} = 1000$ K; curve 3 refers to the case when $T_{ext} = 1250$ K; curve 4 refers to the case when $T_{ext} = 1500$ K. Dashed curves refer to the cases of uniform radiation absorption.

temperature, all of the heat coming to the droplet surface from the gas is spent on evaporation (latent heat), and the net heat penetrating to the liquid phase becomes zero: $Q_L = 0$. In the presence of radiation, however, the droplet surface temperature continues to rise above the wet-bulb temperature. As the surface droplet temperature increases, the heat coming to the droplet surface through convection decreases, but the heat used for vaporization, $\dot{m}L(T_s)$, increases. As a result, the value of Q_L becomes negative, as confirmed by our calculations. At the end of the evaporation period, the total radiation absorption decreases very fast with the droplet radius: $Q_{rad,tot} \sim R_d^{2.5}$, while the heat transferred through the droplet surface, Q_L, decreases relatively slowly being approximately proportional to the droplet radius: $Q_L \sim R_d$. At a certain moment, the total amount of heat going into the droplet interior ($Q_{rad,tot} + Q_L$) becomes negative and $dT_{av}/dt < 0$ in accordance with Eq. (2.6). Therefore the temperature of the irradiated droplet approaches a maximum value, and then decreases toward the wet-bulb temperature of the droplet without radiation. Physically, this resembles the situation where a droplet suspended at room temperature is heated by internal heat sources. Since the vaporization is relatively slow, the droplet temperature will approach some steady-state value, which is higher than the regular wet-bulb temperature. If the internal heat sources are suddenly 'turned-off', the droplet temperature will decrease down to the wet-bulb temperature.

Finally, we compared the results of calculations performed using two extreme: (a) complicated two-dimensional 'extended vaporization model' with detailed consideration of the internal fluid circulation, and the distributed radiation absorption heat source, and (b) very simple one-dimensional 'effective-conductivity' model (k_{eff}-model) with uniform distribution of the internal heat source. Note that the results predicted by the k_{eff}-model with 10 and 100 cells in the radial direction are practically indistinguishable. Exceptionally good agreement between the predictions of these models allows us to recommend using the k_{eff}-model with uniform radiation absorption for spray combustion calculations, including applications for diesel engines.

4. Conclusions

The 'extended' and 'effective-conductivity' models of droplet vaporization developed by Abramzon and Sirignano [2] are generalized to take into account the contribution of thermal radiation and the temperature dependence of liquid fuel properties. In the first model, the convection of liquid is explicitly taken into account, while in the second model the effect of liquid convection on the droplet surface temperature is accounted for by replacing the actual thermal conductivity of liquid by the so called 'effective thermal conductivity'. In both models the contribution of thermal radiation is taken into account based on the simplified model for thermal radiation absorption suggested by Dombrovsky and Sazhin [6]. This model is based on the geometric optics and the MDP_0 approximations, and allows a rather simple description of temperature distribution inside the droplet. Physical properties of diesel fuel are approxi-

mated by those for *n*-dodecane. It is pointed out that the radiation absorption in diesel fuel is generally stronger than in *n*-decane, and it needs to be taken into account in modeling the combustion processes in diesel engines. Weak effect of thermal radiation in *n*-decane droplets, however, may be related to the fact that due to lack of experimental data, absorption coefficient was assumed to be zero at $\lambda < 2.6\,\mu m$. When data were available, the absorption of radiation of *n*-decane was generally less than that of diesel fuel especially in the regions of semi-transparency (λ not close to 3.4 μm). Comparison between the calculations performed using the 'extended vaporization' model and distributed radiation absorption heat source and those based on the 'effective-conductivity' model with the uniform distribution of the internal heat source show exceptionally good agreement between the results. This allows us to recommend using the 'effective-conductivity' model with uniform radiation absorption for spray combustion calculations, including the applications in diesel engines.

References

[1] R. Stone, Introduction to Internal Combustion Engines, New York, MacMillan, 1992.

[2] B. Abramzon, W.A. Sirignano, Droplet vaporization model for spray combustion calculations, Int. J. Heat Mass Transfer 32 (9) (1989) 1605–1618.

[3] W.A. Sirignano, Fluid Dynamics and Transport of Droplets and Sprays, Cambridge University Press, 1999.

[4] S.S. Sazhin, G. Feng, M.R. Heikal, I. Goldfarb, V. Gol'dshtein, G. Kuzmenko, Thermal ignition analysis of a monodisperse spray with radiation, Combust. Flame 125 (2001) 684–701.

[5] P.L.C. Lage, R.H. Rangel, Total thermal radiation absorption by a single spherical droplet, J. Thermophys. Heat Transfer 7 (1) (1993) 101–109.

[6] L.A. Dombrovsky, S.S. Sazhin, Absorption of thermal radiation in a semi-transparent spherical droplet: a simplified model, Int. J. Heat Fluid Flow 24 (2003) 919–927.

[7] R. Kneer, M. Schneider, B. Noll, S. Wittig, Diffusion controlled evaporation of a multicomponent droplet: theoretical studies on the importance of variable liquid properties, Int. J. Heat Mass Transfer 36 (9) (1993) 2403–2415.

[8] M. Burger, R. Schmehl, K. Prommersberger, O. Schäfer, R. Koch, S. Wittig, Droplet evaporation modelling by the distillation curve model: account for kerosene fuel and elevated pressures, Int. J. Heat Mass Transfer 46 (23) (2003) 4403–4412.

[9] R. Clift, J.R. Grace, M.E. Weber, Bubbles, Drops and Particles, Academic Press, New York, 1978.

[10] M. Renksizbulut, M.C. Yuen, Numerical study of droplet evaporation in a high-temperature stream, ASME J. Heat Transfer 105 (1983) 389–397.

[11] P.L.C. Lage, R.H. Rangel, Single droplet vaporization including thermal radiation absorption, J. Thermophys. Heat Transfer 7 (3) (1993) 502–509.

[12] M.C. Yuen, L.W. Chen, On drag of evaporating liquid droplet, Combust. Sci. Technol. 14 (1976) 147–154.

[13] A. Tuntomo, Transport phenomena in a small particle with internal radiant absorption, Ph.D. Dissertation, University of California at Berkeley, Berkeley, CA 1990.

[14] S.S. Sazhin, W.A. Abdelghaffar, E.M. Sazhina, S.V. Mikhalovsky, S.T. Meikle, C. Bai, Radiative heating of semi-transparent diesel fuel droplets, ASME J. Heat Transfer 126 (2004) 105–109 (Erratum 126, 490–491).

[15] E.M. Sazhina, S.S. Sazhin, M.R. Heikal, V.I. Babushok, R. Johns, A detailed modelling of the spray ignition process in Diesel engines, Combust. Sci. Technol. 160 (2000) 317–344.